A simplified method to assess generation of seismic debris for masonry structures

A SIMPLIFIED METHOD TO ASSESS GENERATION OF SEISMIC DEBRIS FOR MASONRY STRUCTURES

Marco Domaneschi[1], Gian Paolo Cimellaro[2] , Gianluca Scutiero[3]

ABSTRACT

Seismic damage simulation at the regional scale provides valuable information that can facilitate decision making and disaster mitigation, reducing both human and economic losses. Building damage assessment after an earthquake event is one of the crucial activities in seismic loss estimation. The amount of generated debris and the associated effects on critical infrastructures are also essential information to evaluate. Indeed, as cascading consequence of debris accumulation, the road network can be interrupted. This entails an overall increase in the average number of people who have difficulty to evacuate, with a significant risk that some residents cannot evacuate at all. This study presents a methodology to assess the area covered by debris generated by the collapse of masonry buildings as function of the geometric characteristics of the structure. The proposed methodology allows the estimation of debris volume and can provide decision-makers with a tool to explore the community response to a disruptive event, quantifying the performance of critical infrastructure and planning better resilience strategies to minimize losses and recovery time.

Keywords: Earthquake; Debris; Masonry; Resilience; Infrastructures, Collapse.

INTRODUCTION

Recently several seismic events hit different regions in the world such as the Central Italy (2016) and the Chiapas' State in Mexico (2017). To reduce social and economic losses following strong ground

[2] Assistant Professor, Department of Structural & Environmental Engineering, Politecnico di Torino, Turin, Italy, E-mail: *marco.domaneschi@polito.it*

[3] Visiting Professor, Department of Structural & Environmental Engineering, University of California Berkeley, USA, E-mail: *gianpaolo.cimellaro@polito.it*

[3]Visiting Student, Department of Structural & Environmental Engineering, University of California Berkeley, USA, E-mail: *gianlucascutiero@berkeley.edu*

motions, the focus has been recently shifted to mitigation and preventive actions to be undertaken before the earthquake occurs [1] [2]. Following the collapse of buildings due to a seismic event, large amounts of debris may be generated, which could constitute a serious obstacle to emergency operations and evacuation [3]. This leads to an overall increase of the average number of people who have difficulty evacuating [4]. In literature few authors have already analyzed the problem of debris generation due to earthquakes. For example, García-Torres et al. [5] and Rafee et al.[6] analyzed the implementation of strategies in debris management after seismic events. Tanikawa et al. [7] examined the losses of buildings and infrastructures following disasters, such as a tsunami and earthquake. However, none of the methodologies mentioned above has been developed and presented in literature to quantify the extent of the *debris area* to determine whether a road is blocked or not.

This work proposes a simplified analytical formula to estimate the debris extension through the numerical simulation of collapse scenarios of buildings that are validated using existing experimental tests. The development of a computational model that can be applied to study the collapse of a masonry building requires specific computational tools. Nowadays, the Finite Element Method (FEM) is the most used numerical tool in the computational structural analysis. However, a few decades ago, another method for the analysis of structures has been developed, the Applied Elements Method (AEM) [8][9]. Experimental tests on a shaking table are analyzed to assess the effectiveness of AEM models in properly reproducing collapses and to highlight the dependence of the solution from the problem's discretization. Then, the extent of *debris area* is determined by numerical simulations within a parametric study of masonry buildings. Finally, a study of how a car might be able to maneuver along a road with different amounts of debris is performed.

METHODOLOGY TO IDENTIFY THE ANALYTICAL FORMULA

This research moves from the identification of a reliable tool that could be employed for performing parametric analyses on masonry building models to reasonably reproduce the structural collapse and the generated debris. With this aim, a preliminary step consists in the calibration of the selected AEM

numeric procedure considering existing laboratory results that has been performed on a shaking table facility. The experimentations are focused on the collapse mechanisms of simple masonry structures.

Following the reliability assessment of the numerical tools, the parametric study has been performed. It consists in a sequence of collapse simulations using AEM considering 81 different masonry buildings with standardized heights and dimensions. The debris volume and extension resulting from the collapse of each building are the output of the parametric analysis and represent a consistent statistic sample that can be used for extrapolating general outcomes.

Different shape areas have been then considered to delimit the debris extension as obtained from the parametric analysis. They are defined by scaling the original dimensions of the building's footprint and taking into account the maximum height of debris that allows for the transit of a standard sized car. Following this procedure, it has been extrapolated a general formula to estimate the debris extension area for masonry buildings as function of their geometric characteristics.

The next sections are devoted to the presentation of the AEM numeric procedure and the building model calibration for performing the subsequent parametric analysis. Then, debris height limit for road serviceability is analyzed and the analytical formula is extrapolated. Finally, a district of a virtual city model is considered to apply the proposed formula and assess debris extension after an earthquake.

THE APPLIED ELEMENT METHOD AND THE MODELS CALIBRATION

The FEM has been the most widely used technique to model continuum mechanical problems. However, some decades ago, the AEM has been developed as a new computational method for the analysis of structures [8][9]. It is a modeling method that adopts the concept of discrete cracking [10]. Through two decades of continuous development, the AEM has been proven to be able to track the structural collapse behavior passing through all stages at increasing loading conditions. E.g. considering the reinforced concrete as a structural constitutive material, it is possible to reproduce the elastic stage, the crack initiation and propagation, steel reinforcement yielding, element separation, collision (contact) with the ground, with other elements and with adjacent structures.

Figure 1 shows the analysis domain of the AEM with respect to the FEM. Although the FEM is accurate and reliable for the analysis of continuum structures, the onset of element separation is difficult to automate and the modeling of debris collision is time-consuming. On the other hand, with AEM, the structure is modeled as an assembly of small elements that virtually subdivide the structure. For example, Figure 2-a depicts the discretization of a concrete frame within the AEM. Each structural component (columns and beams) is subdivided in several discrete elements. A couple of elements is assumed to be connected by one normal and two orthogonal shear springs distributed on the elements adjacent faces, as shown in Figure 2-b. Each group of springs completely represents stresses and deformations for a constitutive material of the composite structure, e.g. reinforced concrete structures contain face distributed springs triples for concrete material and a single triple of springs only for each steel bar. These springs allow also to implement the failure criteria properties associated to the structural component, as discussed in the next subsection. The springs' generation is automatically performed in the AEM software Extreme Loading for Structure [11].

Element separation criteria

The average normal strain is calculated by averaging the absolute values of strains on each face of the elements. When the average strain between these two adjacent faces reaches a threshold called the separation strain – which is specified in the material property – springs between these two faces are removed and it is assumed that these elements behave as two separate rigid bodies for the remaining of the analysis. Separation strain represents the limit at which adjacent elements are totally separated at the connecting face as shown in Figure 3. Therefore, the refinement level of the discretization is a significant parameter to be calibrated to accurate reproduce the structural collapse.

According to Meguro et al. [8], the springs that simulate the steel reinforcement bars in a composite material are removed if the internal stresses reach the failure criteria in Eq. (1).

$$f_u = \sqrt{\sigma^2 + \tau_1^2 + \tau_2^2} \tag{1}$$

where σ, τ_1, τ_2 are respectively the normal and shear stresses and f_u is the unidirectional limit stress of the reinforcement bar. Alternatively, the spring is removed if the internal strains reach the unidirectional limit strain e_u defined in Eq. (2)

$$e_u = \sqrt{\varepsilon^2 + \gamma_1^2 + \gamma_2^2} \tag{2}$$

where ε, γ_1, γ_2 represent respectively the longitudinal and shear strains. One of the features in AEM is the *automatic element contact detection*. Elements may collide each other, separate and collide again. There are three types of collisions: (i) element corner-to-element face, (ii) element edge-to-element edge and (iii) element corner-to-ground [11].

Modeling masonry using AEM

Using the AEM, the brick can be simulated either in a staggered pattern (micro-modeling), in its real configuration, or as homogeneous material (macro-modeling), as shown in Figures 4a and 4b respectively [11][12][13]. The real configuration (Figure 4a) includes the individual bricks in a staggered pattern connected by interface springs with mortar. This option allows to define different characteristics for the material and the mortar. The second option, the macro-modeling simulation (Figure 4b), represents the homogenized version of the wall where a single material is implemented with averaged characteristics (extrapolated from both the brick and the mortar properties).

Calibration of the building models using shaking table tests

A case study conducted by Imai H. et al. [14] on masonry buildings tested on a unidirectional shaking table is analyzed to evaluate the accuracy of the simulation by AEM and the influence of the mesh discretization on the solution. Two houses have been prepared and dynamically tested with fourteen ground motions on a seismic simulator at National Research Institute for Earth Science and Disaster Prevention (NIED-JP) on February, 2011. The AEM methodology has been validated comparing the gable wall displacement at the top of the building subjected to the NS component of 1995 Kobe earthquake [14] that was the only open access data available.

The buildings' geometry is shown in Figure 5. Building *model A* is prepared in compliance with the minimum requirements set in the National Structural Code of the Philippines [15]. The walls are made of 400 × 200 × 150 mm concrete hollow blocks (CHB). The mortar mix has a cement/sand ratio of 1/4 and it has been used both for joining and filling the bricks. The vertical and horizontal reinforcement 10 mm diameter bars are spaced 400 and 600 mm respectively. The building *model B* represents the non-engineered construction of typical houses in the Philippines. Standard material and poor construction implementation are used with 400 × 200 × 100 mm CHBs, filled hollows and joints with the same *model A* mortar mix ratio. Differently from previous building *model A*, uncompact mortar is used for building *model B.* The vertical and horizontal reinforcement 6 mm diameter bars are spaced 600 and 900 mm respectively. This is the common practice in accordance to revelations of local construction workers [14].

In order to reproduce the seismic behavior of the tested structures, it has been essential to deepen the mechanical characterization of the materials. Therefore, compression strength tests have been performed on material specimens of masonry units without reinforcing bars (CHBs filled and joined with mortar) at Mie University (JP). The results are reported in both Figure 6 (stress-strain output) and Table 1 (compressive strength, dimensions, mortar characteristics). Specific tests on mortar only have shown that the compressive strength ranges between 9.5 N/mm^2 and 15.2 N/mm^2. From the performed material characterization, it is highlighted how the application of mortar is a critical aspect of the construction phase because the CHBs themselves has a poor strength.

The shaking table tests have shown structural collapse mechanisms only for *model B* and, consequently, it has been the only one considered in the AEM analysis to study the debris distribution. Indeed, the shaking table tests of the model of building *B* have shown partial collapses using the unscaled Kobe earthquake (Kobe_un) and total collapses for amplification factors larger than 110% (Kobe110). It can be justified by the expected non-ductile response of *model B* with respect to the seismic input. Thus, a small change in the seismic input signal can lead to disproportional consequences such as the collapse.

The masonry walls are implemented through the homogeneous material approach (macro-modeling). This method is used for large-scale models so that mortar joints and brick units are smeared in isotropic (or anisotropic) material [16]. However, although masonry is not homogeneous, this method is able to predict the global behavior of a masonry building and reduce the computational time to perform a large number of simulations.

The material specimens D, E and F reported in Figure 6 and Table 1 refers to *model A* only and they are the only open access data available for the mechanical characterization. The CHBs thickness of building *model B* (100 mm) is smaller than material specimen E (150 mm in Table 1) of *model A*. Consequently, the mechanical properties of specimen E are reasonably higher. As a result, to validate the AEM simulations of *model B* with the experimental shaking table tests, the material parameters are decreased using a back analysis, until the partial collapse at the top of the gable wall during *Kobe_un* is equivalent to that recorded during the experimental tests. The records *Kobe_un* and *Kobe110* have been used for the comparison between the shaking table tests and the numerical simulations. In detail, the following damages have been detected:

- Record *Kobe_un*. East wall: collapse of gable wall; cracking in the upper part of the opening. West wall: collapse of both the gable wall and the upper half part of the same wall. North and South wall: minor cracks.
- Record *Kobe110*. Total collapse.

The compressive ($\boldsymbol{f_m}$) and the shear strength ($\boldsymbol{f_{vk}}$), the elastic (**E**) and shear modulus (**G**) adopted in the AE model are 1.15 N/mm^2, 0.35 N/mm2, 2400 N/mm^2 and 600 N/mm^2 respectively. Figure 7 depicts the comparison between the shaking table tests of *model B* and the AEM simulations. Figure 8 reports the comparison between the AEM simulation and the shaking table test for *Kobe_un* earthquake, where the same time increment for the building collapse is highlighted for both the numerical simulations and the shaking table tests. The test highlights initial minor vibrations of the gable wall, then a discrete jump of 15 cm and another one in the opposite direction of 30 cm at 15 s. The collapse occurs at about 16 s. What happens is that the gable wall initially vibrates to the nearest

centimeter, then moves inwards and then suddenly outwards by 30 cm before collapsing [14]. Since a satisfactory matching is observed between simulations and laboratory tests, the AEM procedure is assumed validated.

Sensitivity analysis and mesh dependence

A sensitivity analysis is performed to evaluate the influence of the mesh discretization. The number of elements in AEM has been reduced and consequently the dimensions of the finite elements have been increased, until the displacement of the gable wall shows significant changes in the dynamic analysis with *Kobe_un* earthquake. Mesh 1, 2, 3 and 4 have been prepared and they consist in about 1500, 900, 120 and 60 elements, with an average size of the mesh discretization of 0.1 × 0.07 m, 0.19 × 0.13 m, 0.6 × 0.4 m, 1.2x0.8 m, respectively. Mesh 1, the most refined one, consists of about 10% less elements with respect to the mesh of the validated AEM model (*validated mesh*).

Following Meguro et al. [8], and as reported in Figure 9, reducing the number of elements corresponds to an apparent increment of the collapse limit threshold. Figure 10 shows the distance from the gable wall of the top brick shown in Figure 8. “Mesh 1” and “Mesh 2” curves show a similar trend with respect to the *validated mesh*. On the contrary, the curves corresponding to “Mesh 3” and “Mesh 4” show that the wall does not collapse.

Finally, “Mesh 2” discretization is selected for the additional numerical simulations in the paper due to the satisfactory balance between computational efforts and reasonable results. In detail, “Mesh 2” consists of 13 elements along the height, 15 elements along the width and one element along the thickness of the building. A time step of 0.005 s is used during the analysis, accordingly to the Applied Science International [11] that indicate it should be in the range 0.0001-0.01 s for the seismic analyses and should be fixed accordingly with the shortest natural vibration period of the model [10].

To evaluated the reliability of the selected Mesh 2 on typical masonry buildings of old Italian centers additional numerical simulations have been performed. In particular, the collapse of the Building G1 with the Irpinia Earthquake (November 23, 1980, Calitri) in Benedetti et al. [17] has been reproduced

by AEM. Figure 11 shows a satisfactory comparison of the simulation results with the physical samples on the shaking table (Figure 12 in Benedetti et al. 1998). The test and building conditions (poor quality of construction) have been fixed accordingly with the original paper. Furthermore, the first two natural frequencies of the G1 building model have been computed and resulted consistent with those estimated in laboratory (2.3 and 3.2 Hz).

PARAMETRIC STUDY

Numerical simulations are performed on 27 buildings groups. Each group consists of three types of buildings with 1, 2 and 3 stories respectively, for a total of 81 models. For each group, the geometric dimensions and the areas of the rectangular footprints are shown in Table 2 with respect to the footprint and the number of floors. Additional general details are the thickness of external walls that is 0.4 m, the thickness of internal wall, 0.2 m and the average room's dimensions that are 4 × 3 m. Each building has a typical distribution of doors at the ground floor and windows at each floor, with an external wall that does not have openings. The considered geometric characteristics of the buildings, such as the wall thickness and the distribution of indoor spaces, are based on the characteristics of a typical masonry building in Central Italy [18][19]. The progressive collapse of each building is simulated through nonlinear time-history analyses using the August 24, 2016 Central Italian earthquake record. Figure 12 reports the ground motion input components and the adopted orientations with respect to the footprint (rotated by 45 degrees around the vertical axis). Therefore, four collapse analyses for each building are computed, but only the one associated to the largest *debris area* (the area essentially occupied by debris) is considered. The mechanical parameters are calibrated accordingly with the current Italian seismic standard on existing masonry (NTC 2008), by selecting the lowest ones to obtain the largest debris area. They are the compressive strength (f_m), the shear strength (f_{vk}), the elastic modulus (E) and the shear modulus (G) equal to 1 N/mm^2, 0.2 N/mm^2, 690 N/mm^2 and 230 N/mm^2 respectively. Figure 13 reports an example of a masonry building model and its collapsed configuration using the AEM.

For each collapsed building a scale factor ε is applied to amplify the building's footprint to delimit and include the debris area. Nevertheless, for small *a/b* ratios of the building's dimensions, the *amplified area* (in yellow in Figure 14 is the building footprint area amplified by the scale factor) is way larger than the area occupied by the orange bricks in Figure 14 (*debris area*), while when the *a/b* ratio is close to one, the difference between the amplified and the debris areas is reduced. To overcome this issue, a *fixed tolerance* of debris volume outside the *amplified area* can been accepted (e.g. 10% tolerance as shown in Figure 13 with the red rectangle) if it does not affect the evacuation procedures and the road transit.

The described procedure is quantitatively implemented in several steps. First the output file of each AEM simulation is imported in a CAD software and then converted in a new script file where the distribution (coordinates) and the volume of the debris are recorded. The next step consists in the use of a computational environment [20] where the debris distribution can be processed and the amplification factor ε of the building footprint is computed.

The implemented MATLAB [20] algorithm needs the evaluation of the *debris area* that is included in a polyline (Figure 15a). Then, different geometries have been considered to delimit the debris area: Figure 15b shows the example of the rectangular shape area, while Figures 15c and 15d show two alternative geometries (i.e. elliptic and circular).

For the rectangular shape, the scale factor ε is uniformly applied to amplify each side of the original building's footprint to delimit and include the debris area. Ellipse axes and the circle radius are scaled to include a fixed percentage of debris, following the same principle as that one used for the rectangular shape. In the circular case, the scale factor is the ratio between the radius and the shortest side of the footprint.

A range between 5 m^3 and 21 m^3 of *debris neglected volume* (volume of debris external to the amplified area) has been selected, with respect to the total masonry building's volumes (Table 3). The *debris neglected volume* is associated to a different percentage of the total masonry building's volume (Table 4), accordingly to the building geometry (footprint area and number of stories).

The implemented MATLAB [20] algorithm computes the scale factor for each building, for each percentage of *debris neglected volume* and for each shape area that delimits the debris (rectangular, elliptical and circular). Table 5 shows an example of the computed output.

ASSESSMENT OF ROAD SERVICEABILITY

The effect of the debris on a car transit is analyzed in this section through the AEM software to define the critical debris level for transit. Therefore, accordingly with the Italian road regulation (art. 2, Decreto Legislativo 30 Aprile 1992, n. 285), a 3.5 m transversal size and 18 m length road is modelled (Figure 16a). The *debris neglected volume* is distributed around the building in the farthest area, where only small masonry particles can be found. The smallest particle in particular has dimensions of a single element (0.3×0.2×0.1 m). Therefore, the minimum height of debris accumulation that can be verified is about 0.3 m.

The test is passed if the vehicle starting from point A reaches point B (Figure 16a) without tire failure. The critical debris volume for transit is assessed by nonlinear time-history analysis. Four scenarios with different debris volumes are simulated (Figure 16b): 25 m^3, 20 m^3, 15 m^3, 10 m^3. The distribution of debris on the road was obtained through a numerical simulation of a building collapse with a side close to the road. Starting from the dispersed volume of debris on the road (25 m^3), the following volumes have been obtained reducing the starting volume according to a function that randomly subtracts elements from the input layout.

The adopted scenarios are coherent with the considered range of *debris neglected volume* as defined in the previous section. The debris is uniformly distributed around the building for squared footprint sides' ratio. Instead, when the lowest sides' ratios are considered, approximately the 80% of this volume is concentrated on a surface next to the longest edges of the footprint (about 40% for each one).

The vehicle is modeled like a rigid body while the coachwork is neglected to reduce the computational efforts. The tire model adopted is 225/45 R17 and, according to Recuero et al. [21], this element is

developed using an isotropic elastic constitutive law, a friction coefficient equal to 0.9, and assuming an internal pressure of 200 kPa. The tire model is fully constrained to the rim at the inner circumference and consists of a 486 solid elements mesh. A tires uniform rotation of two laps per second (10 km/h) along a straight line is assumed. Therefore, the vehicle moves on the road and can change its direction only due to debris' obstacles and the total weight (1300 Kg) of the vehicle is distributed on the four tires. The whole adopted car dimensions are shown in Figure 17. The vehicle model is designed to give the wheels a uniform rotation (40deg). Therefore, if the vehicle finds an obstacle and if this one is too big to be overcome, it varies its trajectory. On the contrary, if the wheel is able to climb on the debris in the simulation it goes up.

The step-by-step direct integration method is used for solving the dynamic problem. The time step is reduced accordingly with the shortest natural vibration period of the model and it consists in 0.003 s [10]. The results show that the car passes from point A to B for both cases 3 and 4 that correspond to 10 m^3 and 15 m^3 of debris, respectively. On the contrary, for cases 1 and 2, the tire failure occurs and the car cannot transit the road. Therefore, the critical limit value for road transit is given by

$$V_{debris} = A_{road} \cdot h_{debris} \leq 15 \tag{3}$$

where A_{road} is the road area; h_{debris} is the minimum height of debris after collapsing equal to 0.3m.

PROPOSED ANALYTICAL FORMULA

Table 4 reports the percentages of debris included in the *rectangular*, *elliptic* and *circular* shapes for all buildings' groups evaluated. For example, one story building with a footprint area of 80 m^2 correspond to 62 m^3 of masonry material (Table 3). So, for example, when 10% debris is neglected it means that 6.2 m^3 are not included in the rectangular, elliptic or circular shape area and such neglected debris' volume remain outside the shape area. The *error* adopted variable is defined as

$$error = \frac{\left(A_p - A_s\right)}{A_p} \tag{4}$$

where A_p is the area limited by the polyline (Figure 15a); A_s is the area limited by the selected fixed shapes (e.g. Figure 15b, c, d).

Table 6 shows the percentages of debris inside the shape area, so that the neglected debris is always below the upper threshold of 15 m^3. Therefore, the shape area defines exclusively the space where the car transit is not possible.

This condition is also the essential goal of this paper because it allows to identify the roads that can be interrupted due to collapse of adjacent buildings.

Figures 18-20 show the results in terms of buildings' a/b ratios vs *errors*. Considering the circular shape (Figure 18), it can be noted how the error is larger for low ratios but decreases for unitary (squared) ratios. Elliptical shape (Figure 19) shows lower errors' levels with respect to the circular one, while the rectangular shape (Figure 20) highlights slightly better results with respect to the elliptic one. Therefore, the rectangular shape has been selected to develop the proposed formulation.

The results of Figure 20 are analyzed and interpolated using least square fit methods [22]. The preliminary analyses have been focused on the identification of the best fitting surface and the variables, functions of the building characteristics, that allows to minimize the residuals.

The best fitting solution of the experimental points is shown in Figure 21a. It consist in a plane in the 3D reference system where the sides ratio of the rectangular footprint $\left(\frac{a}{b}\right)$ is reported on the *x* axis, the function $\left(\frac{A_f}{V_b}\cdot\frac{h_b^2}{a}\right)$ on the *y* axis and the scale factor (ε) on the vertical axis. A_f is the footprint area of the building, h_b is the total height of the building, V_b is the total masonry volume of the building. As it can be observed, the variables *x* and *y* are functions of the independent characteristics of the considered building (a, b, h_b, A_f, V_b). The proposed solution has been identified as the optimal one because it allows to reduce the difference between the observed values and the estimated ones at the minimum (Figure 21b).

Residuals tests have been also performed to verify the reliability of the model. Normality of the

residuals is validated by Shapiro-Wilk test [23] that confirms the normality hypothesis as shown in Figure 22a. While, in the second test (Figure 22b) the predicted residuals are satisfactorily compared with the predicted values to validate the homoscedasticity hypothesis [24].

Finally, the formula to determine the rectangular shape amplification factor (ε) is given by

$$\varepsilon = 1.228 + 0.07869 \cdot \left(\frac{a}{b} \right) + 0.05626 \cdot \left(\frac{A_f}{V_b} \cdot \frac{h_b^2}{a} \right) \tag{5}$$

Additional simulations for 1-story building of 80 m^2 are performed to evaluate the possible variations of *debris area* extension due to the variation (improvement) of the material strength (Table 7).

According to NTC (2008) [25], the *P1* set represents the mechanical parameters used for all the presented collapse simulations, while the *P2* set represents new mechanical parameters that can be used for additional simulations. Table 8 reports the comparison between the debris areas computed by *P1* and *P2* parameters. As expected, the results associated to *P1* show larger debris areas with respect to those ones obtained with *P2* parameters. This means that the proposed formula with the lowest strength parameters predicts the worst debris' extension condition. Thus, it is to be intended given the seismic intensity and the building material properties.

EXAMPLE OF APPLICATION

The term "*virtual city*" is used to describe *a two or three-dimensional computer-generated environment that can be explored and interacted* [26]. This can be useful for damage and resilience assessment and could support both designers and policy makers during the decision-making process.

A district of a virtual city model, called Ideal City, freely inspired to the city of Turin in Italy, is herein considered to apply the proposed formula and to assess the area covered by the debris after a strong ground motion [27][28]. The district is characterized by masonry building with compatible geometries for the application of the proposed formula. Considering the earthquake that hits the community and damages the built environment, the resulting debris distribution can be predicted for evaluating its effect on the transportation network. It can be useful to evaluate the community preparedness and its

response to the disaster with the aim of implement the necessary improvements. A numerical code developed in MATLAB [20] has been used to evaluate the debris extension through the proposed formula and to assess to what extent the transportation network can be available for emergency operations. The procedure provides a graphical output showing the interaction of the debris with the transportation network (Figure 23). This procedure can be applied to provide to policy and decision-makers a valuable tool to explore and assess how their community can respond to a disruptive event.

CONCLUDING REMARKS

In earthquake-affected areas, the debris accumulation subsequently to a disruptive earthquake can be problematic for the transportation network, the emergency operations and the evacuation process. The methodology presented in this paper provides an estimation of the area occupied by the debris due to masonry buildings' collapse after a strong ground motion.

This paper presents a parametric study of different collapse scenarios for masonry buildings using numerical simulations that are validated using existing experimental tests performed on a shaking table.

The results of the numerical simulations are interpolated and a simplified formula is presented to estimate the area occupied by the debris produced by the collapse of the masonry buildings. The formula is based on the geometric parameters of the structure.

Furthermore, the interaction between the vehicles transiting on a road link and the debris is investigated, establishing the maximum volume of debris occupying the road that allows the passage of a car.

The proposed formula can be used to predict whether a road is accessible and the transportation network is functional. For example, it can be applied on a large-scale city model to evaluate the resilience of the road network after the collapse of the masonry buildings. Indeed, it can be an element of an emergency management tool that can be used to develop evacuation plans and to assess the preparedness of a community in managing disasters. Furthermore, it could be also useful for the post-

disaster waste management plan that will be triggered immediately after a seismic event, allowing rapid removal and relocation of debris to facilitate the rescue of victims.

ACKNOWLEDGEMENTS

The research leading to these results has received funding from the European Research Council under the Grant Agreement n° 637842 of the project IDEAL RESCUE-Integrated Design and Control of Sustainable Communities during Emergencies. The National Research Institute for Earth Science and Disaster Prevention (NIED - Japan) who made available the experimental for this research data is gratefully acknowledged. Applied Science International LLC, USA is also acknowledged.

Professor Stephen Mahin from the University of California Berkeley actively participated to the research and his invaluable contribution is gratefully acknowledged by the authors.

References

[1] Cimellaro, G. P., et al. (2010). "Framework for analytical quantification of disaster resilience." *Engineering Structures* 32(11): 3639–3649.

[2] Cimellaro, G. P., Renschler, C., Reinhorn, A. M., and Arendt, L. (2016b). "PEOPLES: a framework for evaluating resilience." *Journal of Structural Engineering, ASCE*, 142(10), 1-13 DOI: 10.1061/(ASCE)ST.1943-1541X.0001514.

[3] Hirokawa N, Osaragi T, (2016) Earthquake disaster simulation system: Integration of models for building collapse, road blockage, and fire spread, Journal of Disaster Research, 11(2): 175-187.

[4] Goretti A, Sarli V., (2006) Road Network and Damaged Buildings in Urban Areas: Short and Long-term Interaction, Bulletin of Earthquake Engineering, 4(2): 159-175.

[5] García-Torres, S., Kahhat, R., Santa-Cruz S. (2017). Methodology to characterize and quantify debris generation in residential buildings after seismic events, *Conservation and Recycling*, 117, pp. 151-159.

[6] Rafee, N., Karbassi, A.R., Nouri, J., Safari, E., Mehrdadi, M., (2008). Strategic management of municipal debris aftermath of an earthquake. *Int. J. Environ. R*es. 2 (2), 205–214.

[7] Tanikawa, H., Managi, S., Lwin, C.M., (2014). Estimates of lost material stock of buildings and roads due to the Great East Japan Earthquake and tsunami. *J. Ind. Ecol*. 18 (3), 421–431

[8] Meguro K. & Tagel-Din H. (2000) “Applied element method for structural analysis: theory and application for linear materials. *Structural* Eng./Earthquake Eng. JSCE, Vol. 17, No. 1, 21s-35s.

[9] Meguro K., (2001) “Applied element method: a new efficient tool for design of structure considering its failure behaviour”, Institution of Industrial Science (IIS), The university of Tokyo, Japan, September, pp. 1-20.

[10] Domaneschi, M. (2012). "Experimental and numerical study of standard impact tests on poly-propylene pipes with brittle behavior. " *Journal of Engineering Manufacture, Proc. IMechE Part B*, 226(12), 2035–2046. DOI: 10.1177/0954405412461983.

[11] Applied Science International, LLC (2017), *Extreme loading for structures Theoretical Manual.*

[12] Chácara, C., Mendes, N. and Lourenço, P.B. (2017), "Simulation of Shake Table Tests on Out-of-Plane Masonry Buildings. Part (IV): Macro and Micro FEM Based Approaches", *International Journal of Architectural Heritage*, 11 (1): 103-116.

[13] Lourenço, P.B. (1996), Computational strategies for masonry structures. Delft, The Netherlands: Delft University.

[14] Imai, H., Minowa, C., Lanuza, A.G., Penarubia, H.C., Narag, I.C., Soridum, R.U., Okazaki, K., Narafu, T., Hanazato, T., Inoue, H. (2015) A full-scale shaking table test on philippine concrete hollow blocks (CHB) masonry houses, *Journal of Disaster Research*, 10 (1), pp. 113-120.

[15] NSCP_2010. National Structural Code of the Philippine 2010. Volume I, Buildings, Towers and other vertical structures: Association of Structural Engineers of the Philippines, Inc. (ASEP); 2010.

[16] Lopez, J., Oller, S., Oñate, E. and Lubliner, J. (1999), "A homogeneous constitutive model for masonry", Int. J. Numer. Meth. Engng., 46: 1651–1671.

[17] Benedetti, D., Carydis, P. and Pezzoli, P. (1998), "Shaking table tests on 24 simple masonry buildings", Earthq. Eng. Struct. D., 27: 67-90.

[18] Cimellaro, G. P., Chiriatti, M., Reinhorn, A. M., Tirca, L. (2012). "Emilia Earthquake of May 20th, 2012 in Northern Italy: rebuilding a resilient community to multiple hazards." MCEER Technical Report –MCEER-12-0009, MCEER, State University of New York at Buffalo (SUNY), Buffalo, New York (http://mceer.buffalo.edu/pdf/report/13-0006.pdf).

[19] Cimellaro, G. P., Chiriatti, M., Roh, H., Reinhorn, A. M. (2014). "Seismic performance of industrial sheds and liquefaction effects during May 2012 Emilia Earthquakes sequence in

Northern Italy." *Journal of Earthquake and Tsunami*, 8(2), 23, DOI: 10.1142/S1793431114500092.

[20] Matlab R2017b (2017), The MathWorks, Inc., Natick, Massachusetts, United States.

[21] Recuero A., Serban R., Peterson B., Sugiyama H., Jayakumar P., Negrut D. (2017) A high-fidelity approach for vehicle mobility simulation: Nonlinear finite element tires operating on granular material, In *Journal of Terramechanics*, Volume 72, Pages 39-54, ISSN 0022-4898, https://doi.org/10.1016/j.jterra.2017.04.002.

[22] Table Curve 3D, SYSTAT Software Inc., 1993-2002

[23] Shapiro S.S. & Wilk M. B. (1965), An Analysis of Variance Tests for Normality, Biometrika, Vol. 52, pp. 591-611.

[24] Anderson, T. W.; Darling, D. A. (1952), Asymptotic Theory of Certain "Goodness of Fit" Criteria Based on Stochastic Processes. Ann. Math. Statist. 23, no. 2, pp. 193-212.

[25] Norme Tecniche per le Costruzioni – NTC (2008), *D.M. 14 Gennaio 2008*

[26] Marasco S, Zamani-Noori A, Cimellaro GP. Keynote Lecture: Resilience Assessment for the Built Environment of a Virtual City. 6th International Conference on Computational Methods in Structural Dynamics and Earthquake Engineering (COMPDYN2017). 15-17 June 2017, Rhodes Island, Greece2017.

[27] Marasco S, Cimellaro GP. A new energetic-based ground motion selection and modification method limiting the dynamic response dispersion and preserving the median demand. *Bulletin of Earthquake Engineering.* 2017; DOI: 10.1007/s10518-017-0232-5:1-21.

[28] Marasco, S., Noori, A.Z. and Cimellaro, G.P. (2017), "Resilience assessment for the built environment of a virtual city", COMPDYN 2017 - Proceedings of the 6th International Conference on Computational Methods in Structural Dynamics and Earthquake Engineering, 1, 2043-2055. Rhodes Island; Greece; 15 June 2017 through 17 June 2017. DOI: 10.7712/120117.5548.18180.

List of Tables

List of Figures

Table 1. Material specimens of masonry unit (CHBs filled and joined with mortar).

	CHB	**Reinforcing bar**	**Mortar**		**Compressive test**
	Thickness		Mixing ratio	Compaction	Compressive strength
Specimen D	6 inch, 150 mm	None	1 cement : 4 sand	Compacted	4.40 N/mm^2
Specimen E	6 inch, 150 mm	None	1 cement : 4 sand	Not Compacted	1.42 N/mm^2
Specimen F	4 inch, 100 mm	None	1 cement : 4 sand	Compacted	2.52 N/mm^2

Table 2. Analyzed buildings' groups with rectangular footprint dimensions and different floors.

Group	a[m]	b[m]	a/b ratio	Area [m^2]
1	4	20	0.2	80
2	4.9	16.3	0.3	79.9
3	5.7	14.1	0.4	80.4
4	6.3	12.6	0.5	79.4
5	6.9	11.5	0.6	79.4
6	7.5	10.7	0.7	80.3
7	8	10	0.8	80
8	8.5	9.4	0.9	79.9
9	8.9	8.9	1	79.2
10	8	40	0.2	320.0
11	9.8	32.6	0.3	319.5
12	11.4	28.2	0.4	321.5
13	12.6	25.2	0.5	317.5
14	13.8	23	0.6	317.4
15	15	21.4	0.7	321.0
16	16	20	0.8	320.0
17	17	18.8	0.9	319.6
18	17.8	17.8	1	316.8
19	12	60	0.2	720.0
20	14.7	48.9	0.3	718.8
21	17.1	42.3	0.4	723.3
22	18.9	37.8	0.5	714.4
23	20.7	34.5	0.6	714.2
24	22.5	32.1	0.7	722.3
25	24	30	0.8	720.0
26	25.5	28.2	0.9	719.1
27	26.7	26.7	1	712.9

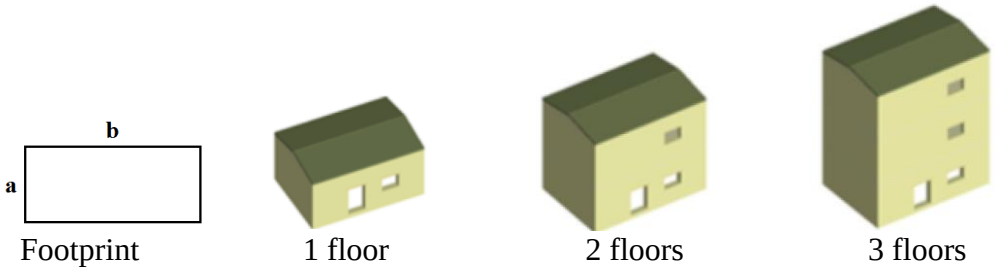

Table 3. Buildings average volumes.

	1 Story	**2 Stories**	**3 Stories**
Area: 80 m^2	62 m^3	110 m^3	158 m^3
Area: 320 m^2	147 m^3	245 m^3	342 m^3
Area: 720 m^2	259 m^3	405 m^3	526 m^3

Table 4. Considered percentages of included debris with respect to the footprint area (80, 320, 720 m^2) and the number of stories.

	1 Story	**2 Story**	**3 Stories**
Area: 80 m^2	100%	100%	100%
	90%	90%	95%
	80%	80%	92.50%
	70%	70%	90%
Area: 320 m^2	100%	100%	100%
	95%	97.50%	98%
	90%	95%	96%
	80%	92.50%	94%
Area: 720 m^2	100%	100%	100%
	97.50%	98.80%	99.30%
	95%	97.60%	98.60%
	92.50%	96.40%	97.90%

Table 5. Example MATLAB code output for 100% included debris (80 m^2 footprint area and 3 stories).

a/b ratio	**Percentage internal points**	***Debris Area* polyline**	***Debris Area* rectangle**	***Debris Area* ellipse**	***Debris Area* circle**	**Scale factor rectangular shape**	**Scale factor ellipse shape**	**Scale factor circular shape**
0.2	100 %	911 m^2	5751 m^2	4098 m^2	3002 m^2	8.48	8.07	7.73
0.3	100 %	901 m^2	5731 m^2	4084 m^2	2931 m^2	8.47	8.07	6.25
0.4	100 %	445 m^2	1385 m^2	987 m^2	1084 m^2	4.15	3.95	3.26
0.5	100 %	374 m^2	910 m^2	649 m^2	686 m^2	3.39	3.23	2.35
0.6	100 %	332 m^2	730 m^2	521 m^2	695 m^2	3.03	2.89	2.15
0.7	100 %	321 m^2	736 m^2	525 m^2	697 m^2	3.03	2.89	1.98
0.8	100 %	317 m^2	961 m^2	685 m^2	666 m^2	3.41	3.3	1.84
0.9	100 %	313 m^2	954 m^2	673 m^2	655 m^2	3.44	3.3	1.7
1	100 %	311 m^2	961 m^2	685 m^2	649 m^2	3.49	3.32	1.62

Table 6. Percentage of internal points.

	1 Story	**2 Stories**	**3 Stories**
80 m^2	80%	90%	92.5%
320 m^2	95%	97.5%	98%
720 m^2	97.5%	98.8%	99.30%

Table 7. Mechanical properties from *P1* set of parameters to the new *P2* one (NTC 2008).

P1					**P2**			
f_m **[N/cm²]**	f_{vk} **[N/cm²]**	**E [N/cm²]**	**G [N/cm²]**	➡	f_m **[N/cm²]**	f_{vk} **N/cm²]**	**E [N/cm²]**	**G [N/cm²]**
100	2.0	690	230		200	3.5	1020	340

Table 8. Comparison between *P1* and *P2* areas.

Ratio	**Area P1 [N/m^2]**	**Area P2 [N/m^2]**
0.2	396	229
0.3	317	194
0.4	445	292
0.5	305	247
0.6	376	329
0.7	253	231
0.8	353	337
0.9	345	321
1	353	341

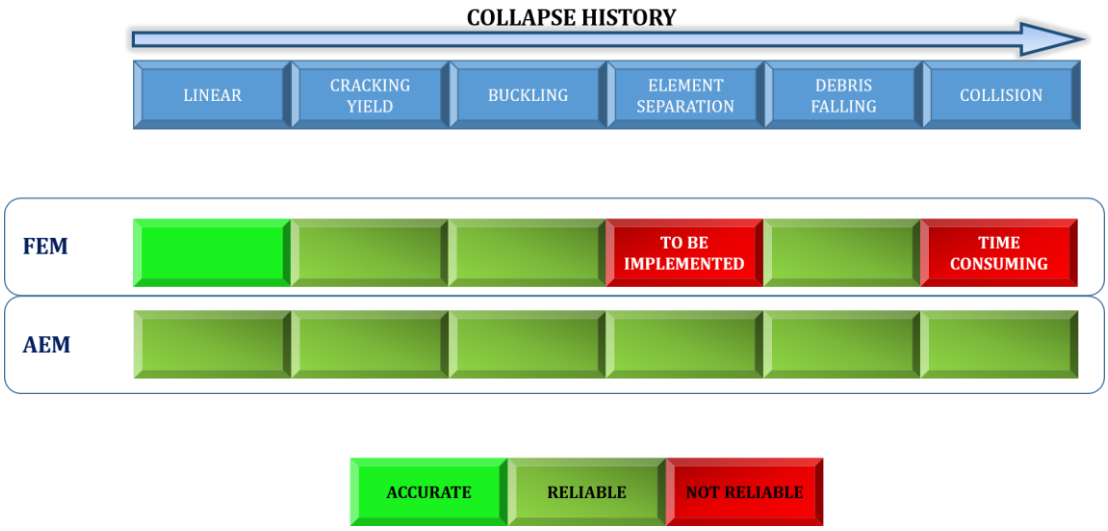

Figure 1. Comparison between AEM and FEM.

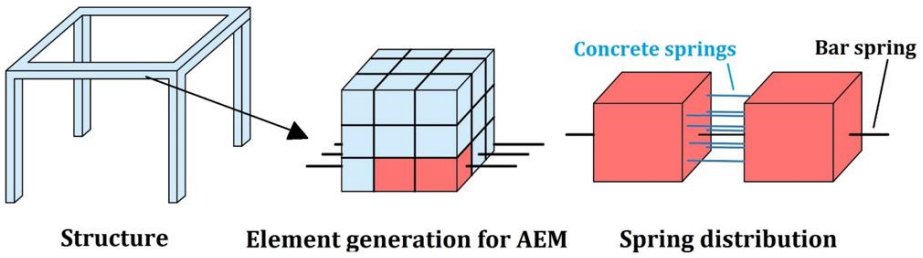

(a)

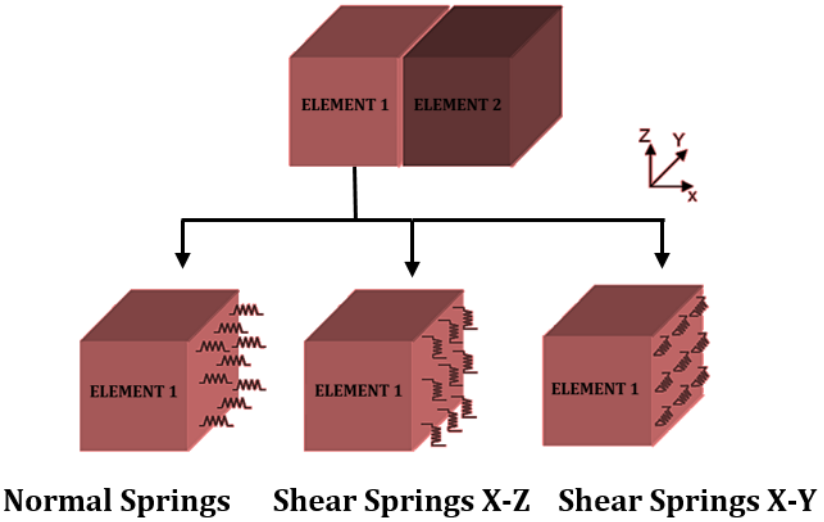

(b)

Figure 2. The AEM: (a) discretization, (b) spring interaction between elements.

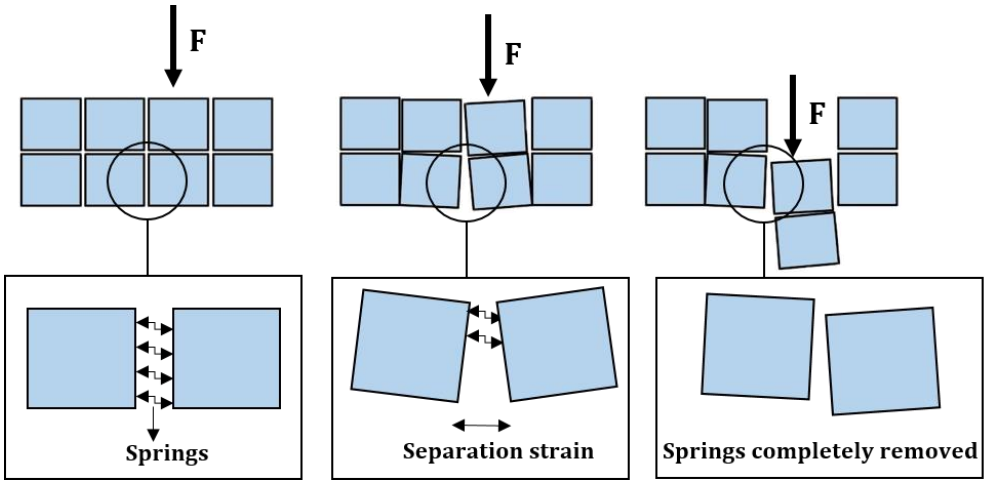

Figure 3. Phases of the separation mechanism.

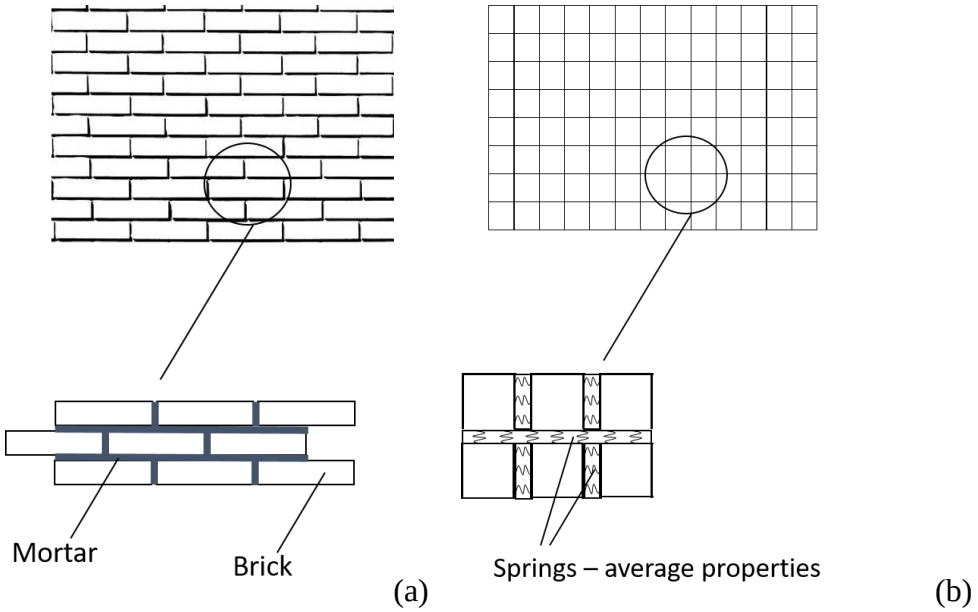

Figure 4. Different meshing for masonry (Applied Science Interational 2017). (a) Staggered pattern (micro-modeling). (b) Homogeneous material (macro-modeling).

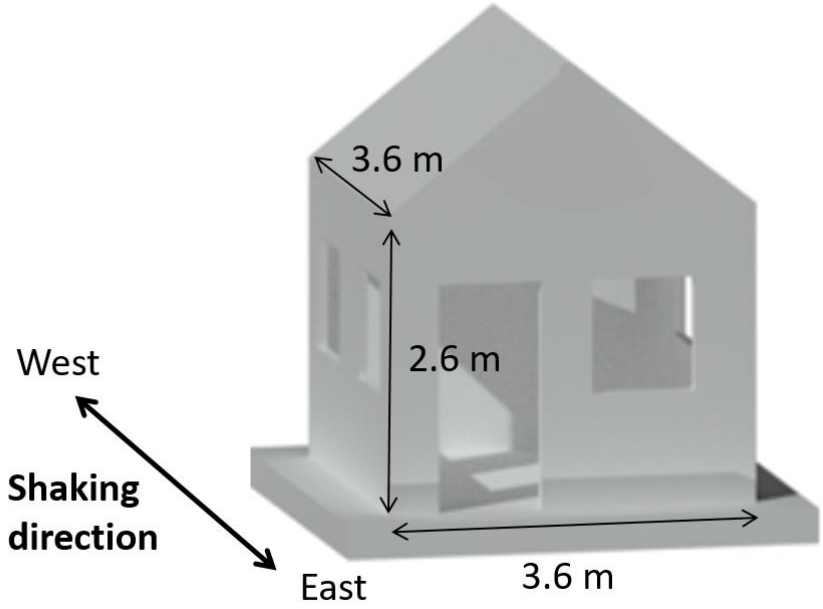

Figure 5. Isometric views of Buildings' geometry with dimensions.

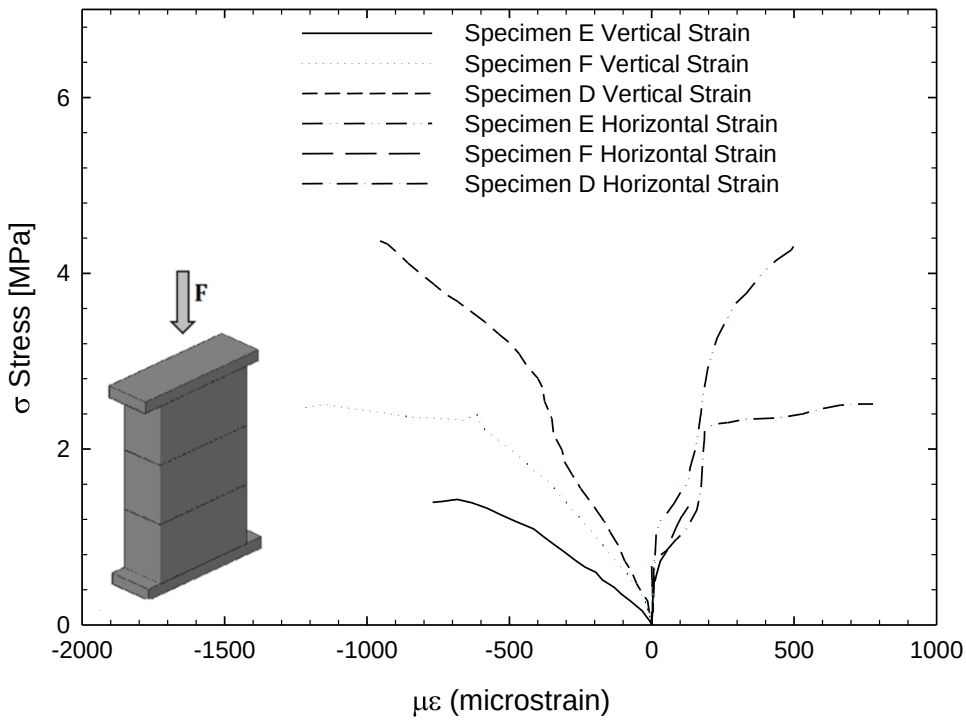

Figure 6. Compressive test results for *Model A.*

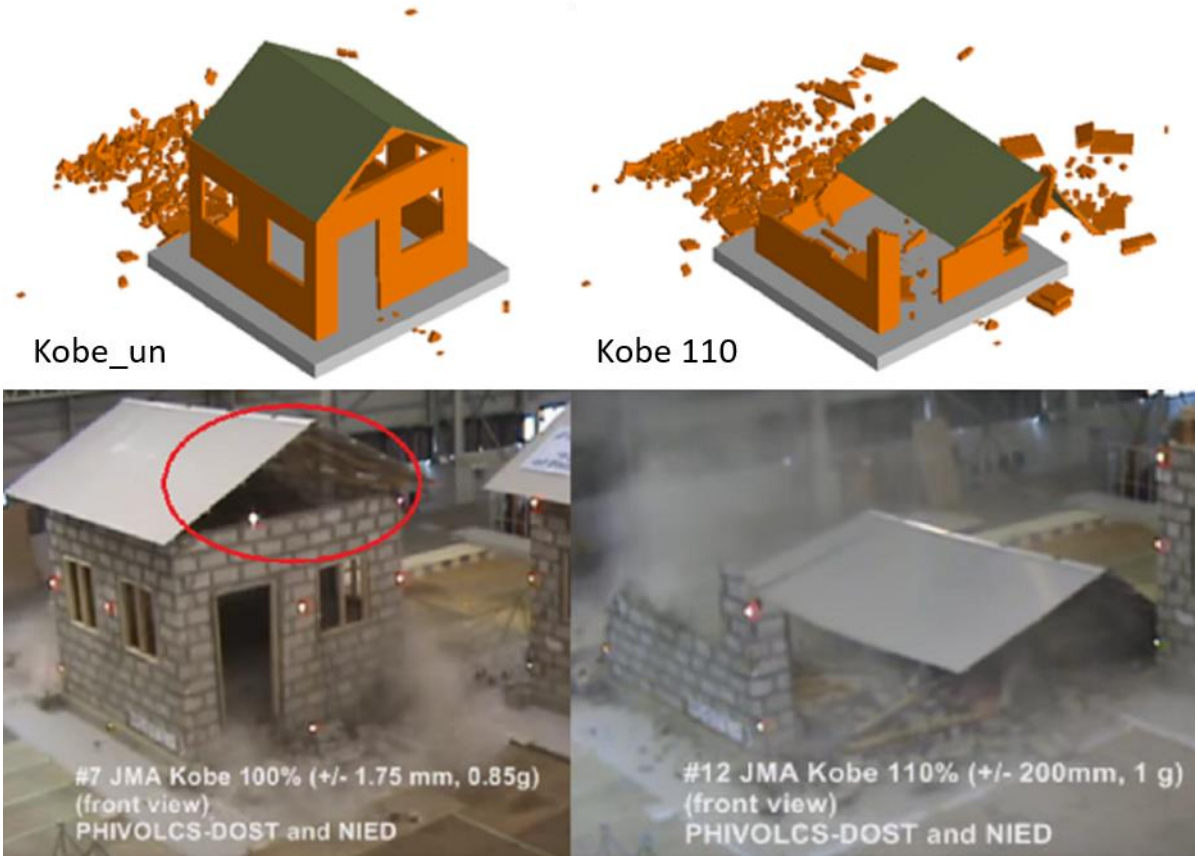

(a) (b)

Figure 7. Comparison between experimental model B and AEM numerical model. *Kobe_un* record (a) and *Kobe110* record (b).

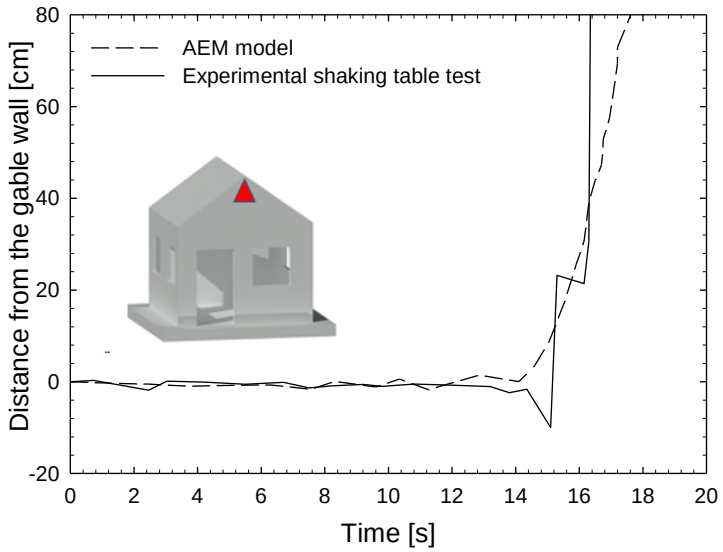

Figure 8. Gable wall displacements during *Kobe_un* record. Comparison between the AEM simulation and the shaking table test.

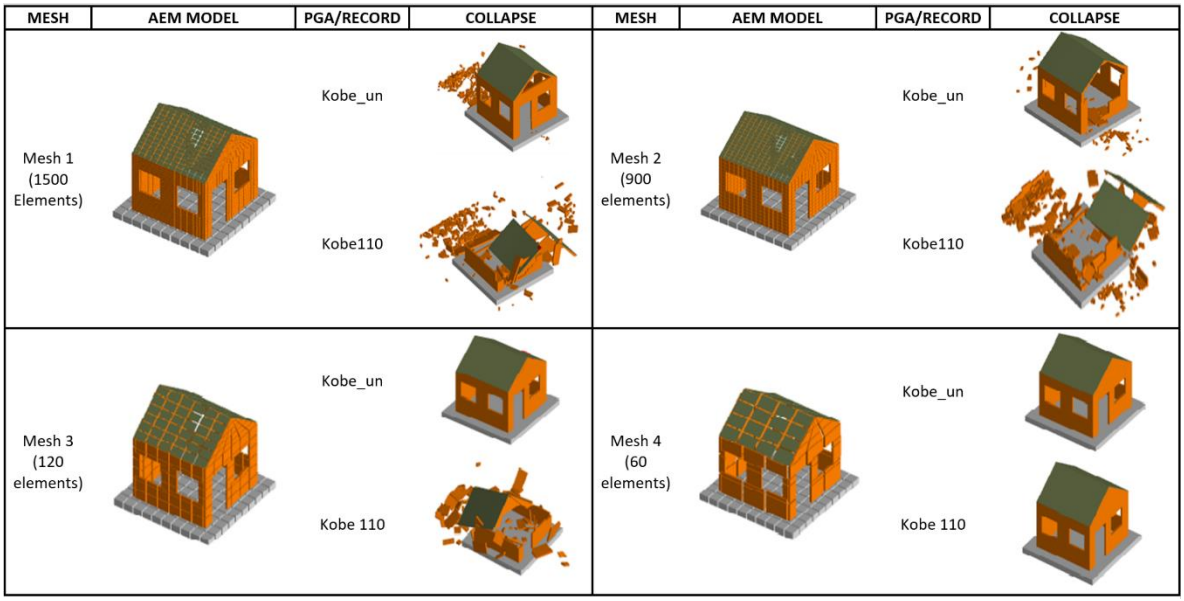

Figure 9. Different meshing of AEM model

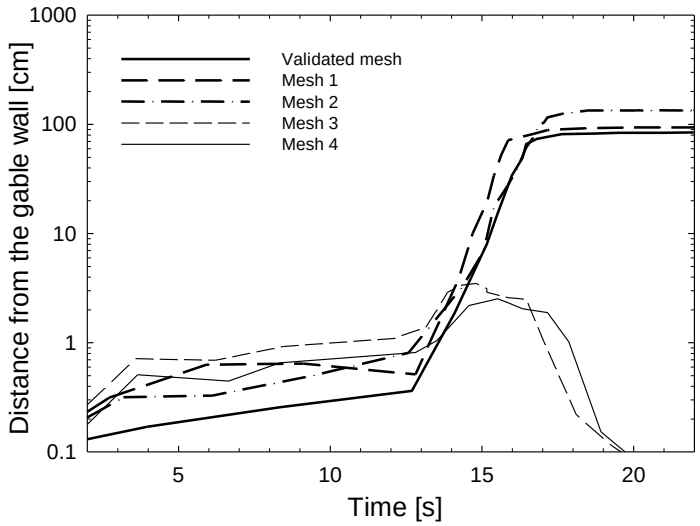

Figure 10. Displacement of gable walls at the top for different mesh sizes.

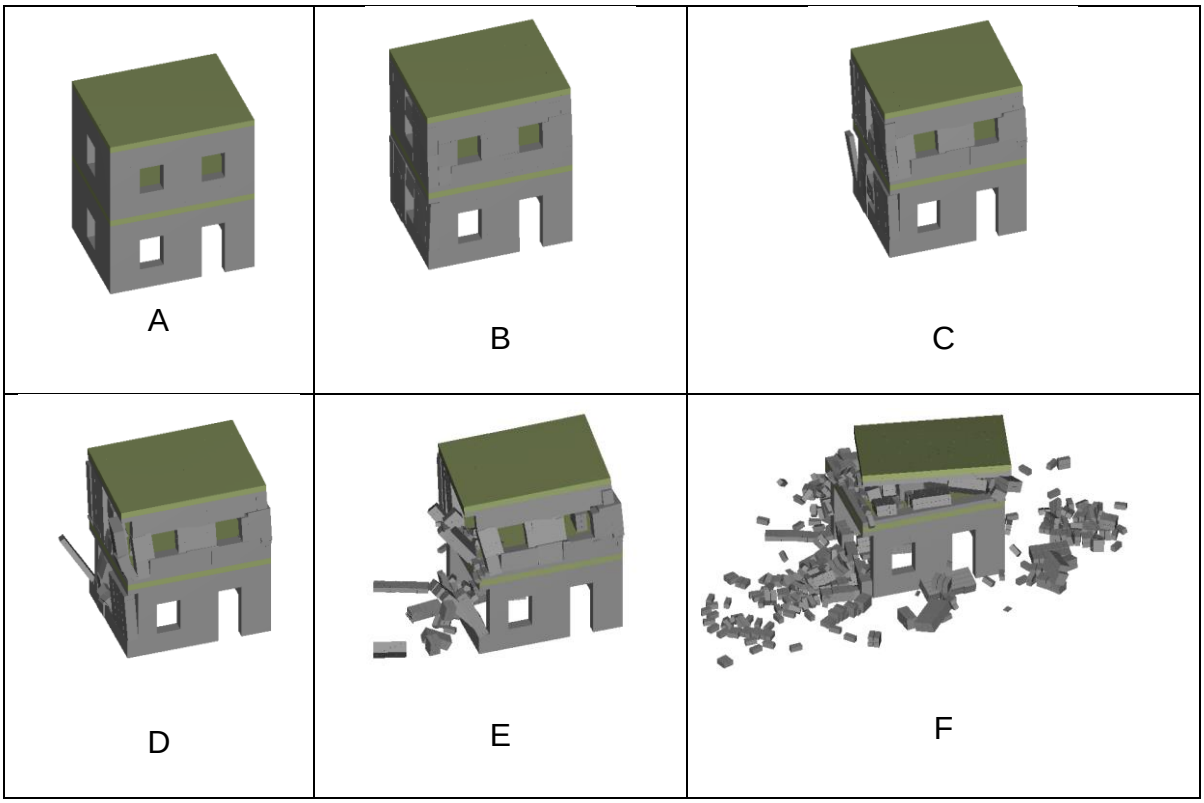

Figure 11. Reproduction of G1 building's collapse in Benedetti et al. [17] (Figure 12 A-F).

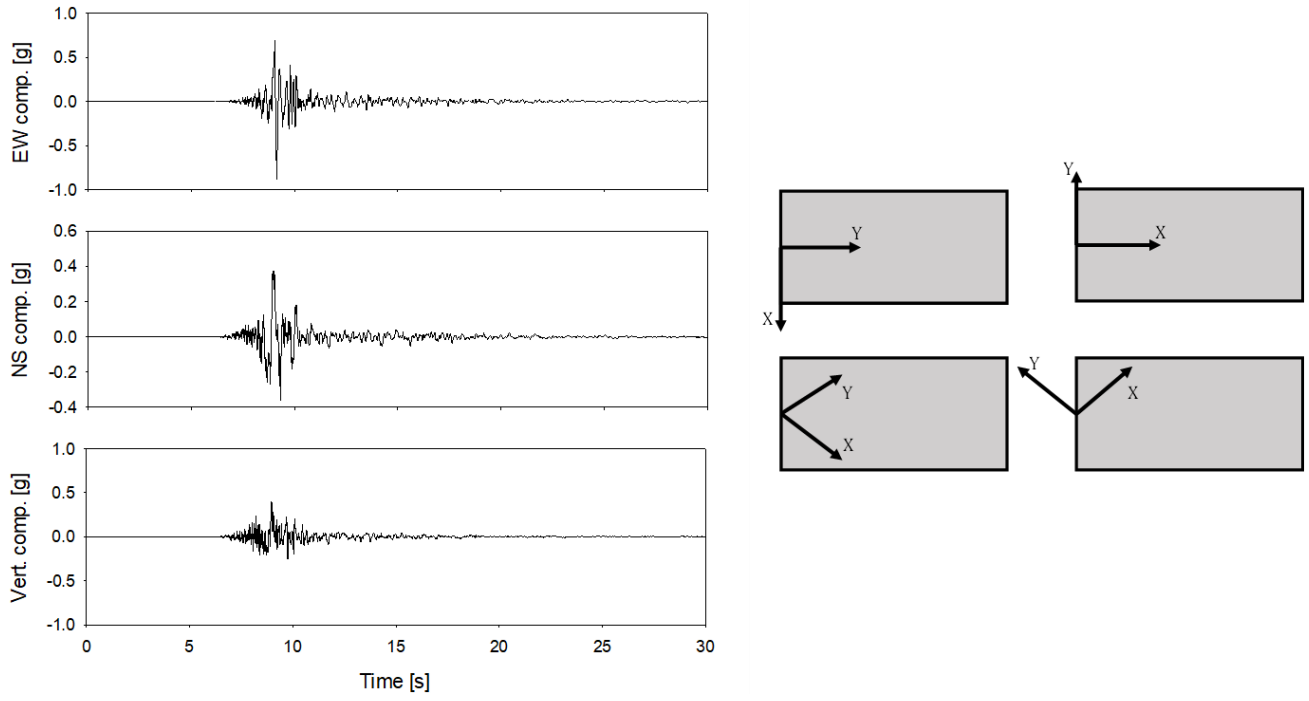

(a) (b)

Figure 12. Accelerogram components of Central Italian Earthquake (Amatrice August 24th, 2016) (a) and earthquake directions (b).

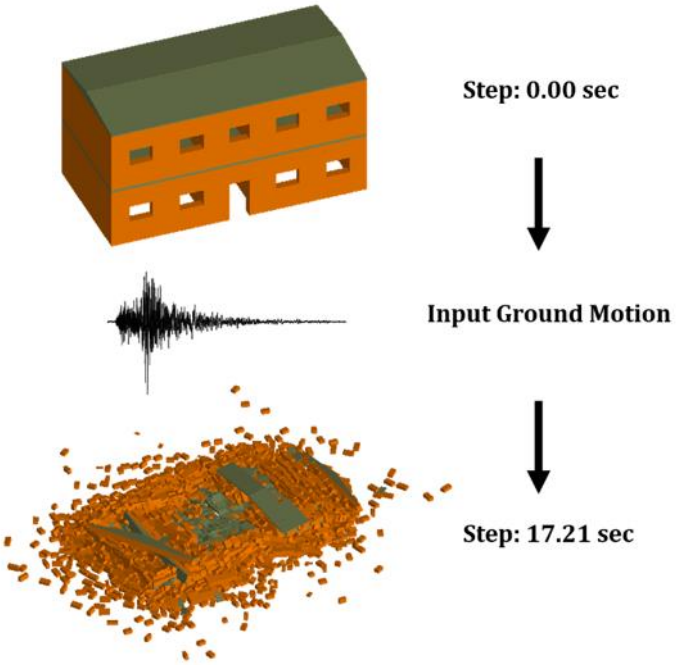

Figure 13. Example of AEM simulation for a typical masonry building in Central Italy.

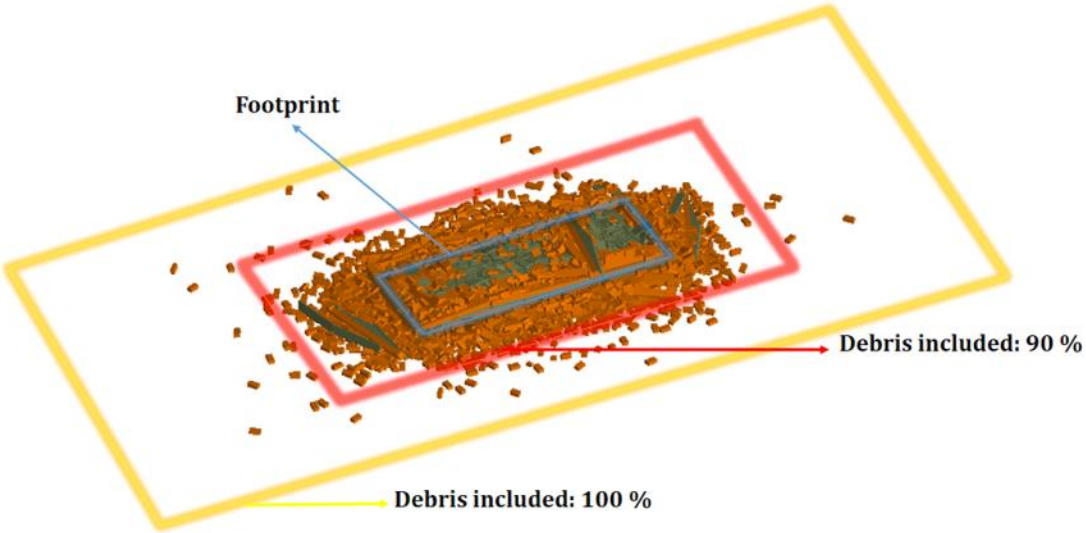

Figure 14. Footprint area and amplified area.

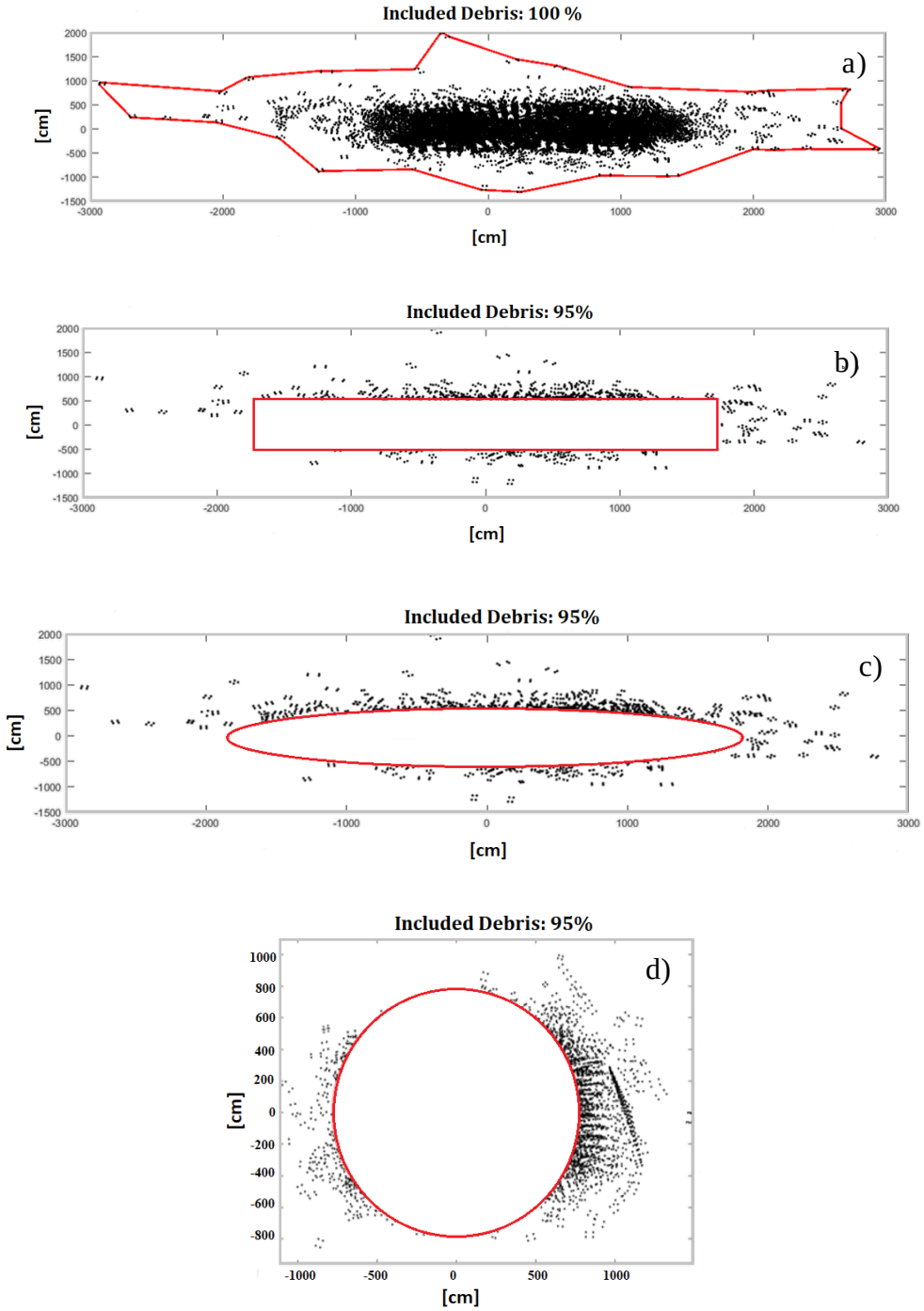

Figure 15. (a) Polyline area with 100% debris included; (b) Rectangular shape amplified area; (c). Elliptic shape amplified area and (d) circular shape amplified area.

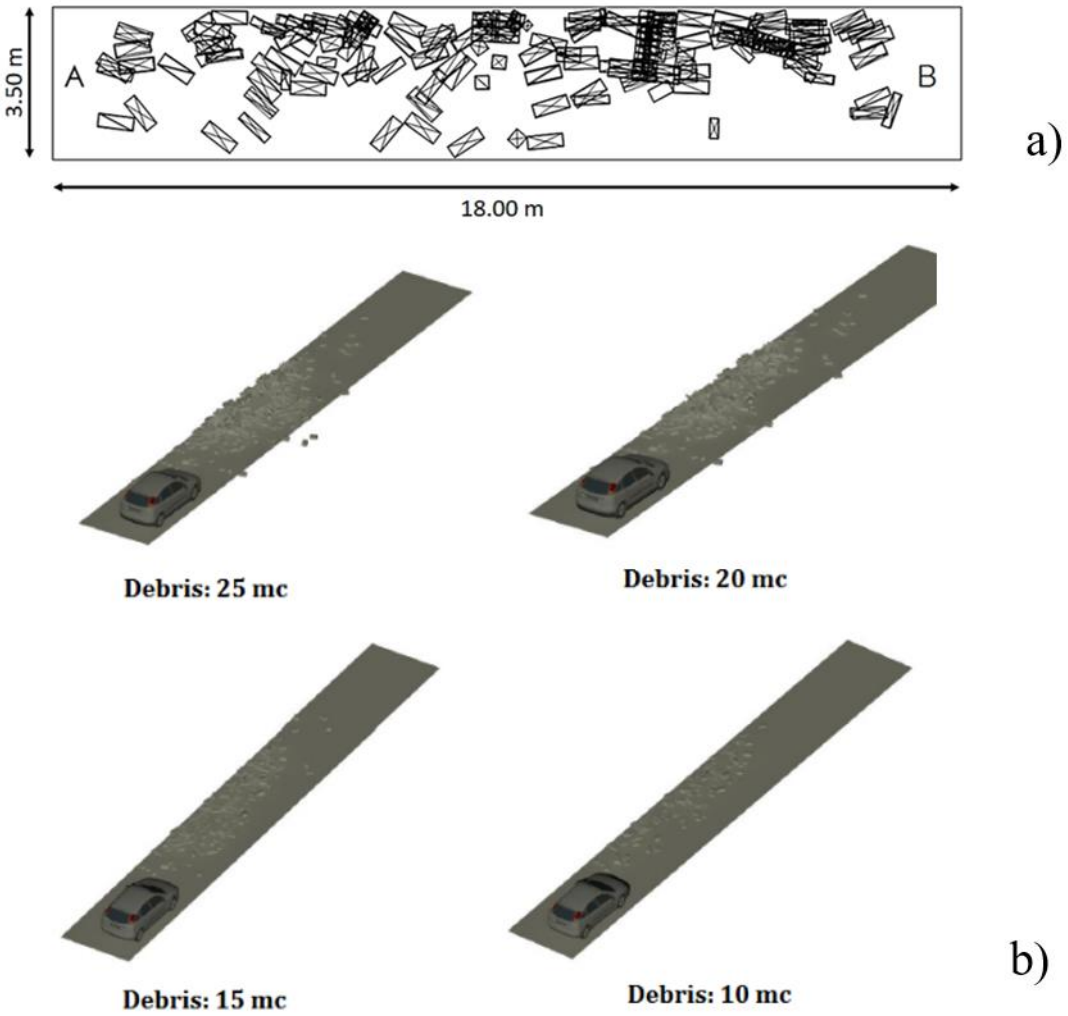

Figure 16. Road dimensions (a). Vehicle passage simulation with respect to the debris' volume (b).

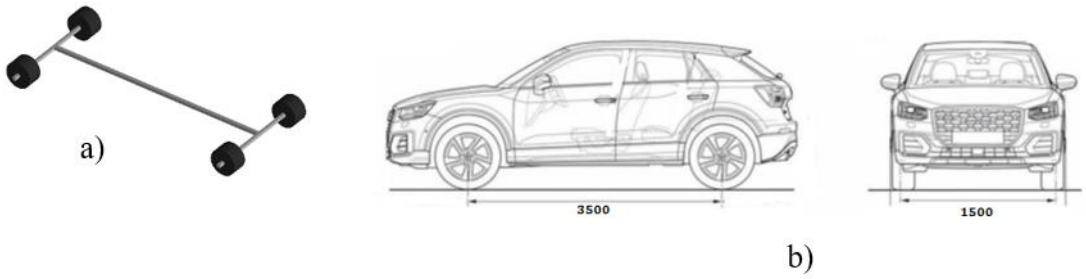

Figure 17. AEM car model (a) and dimensions (b).

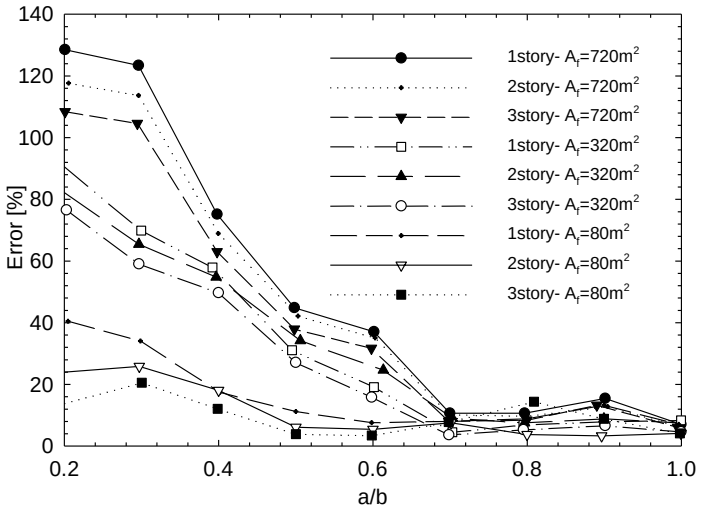

Figure 18. *Error* vs a/b (Circular shape).

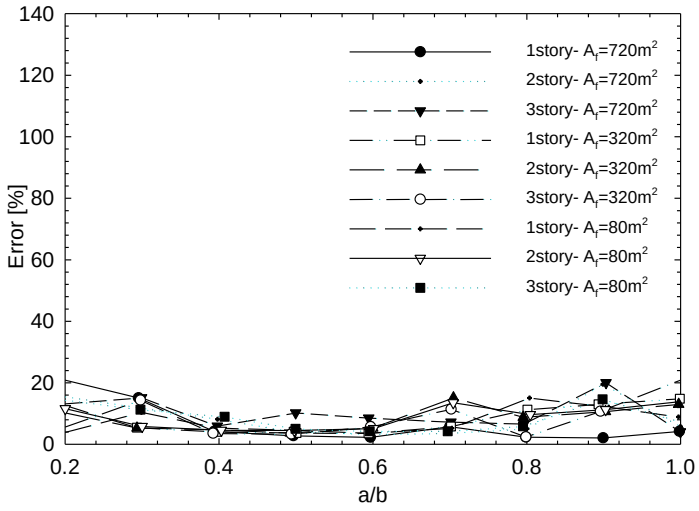

Figure 19. *Error* vs a/b (Elliptical shape).

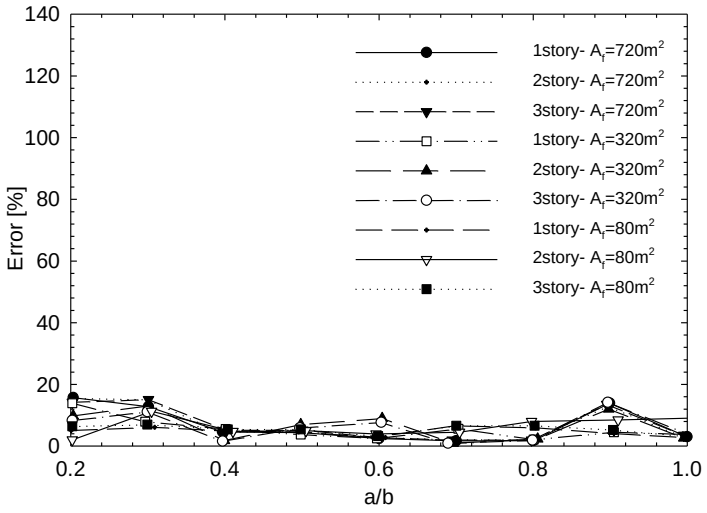

Figure 20. *Error* vs a/b (Rectangular shape).

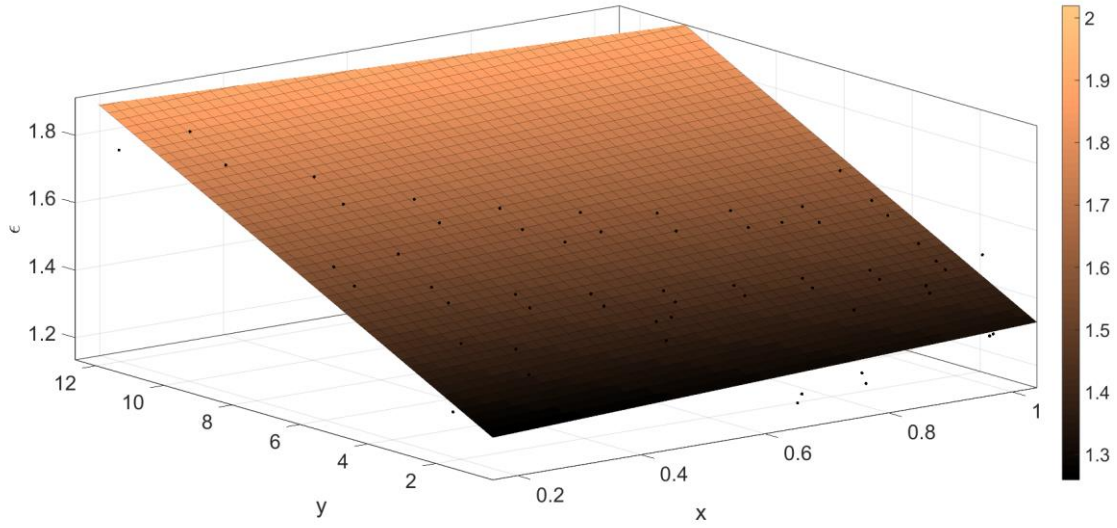

(a)

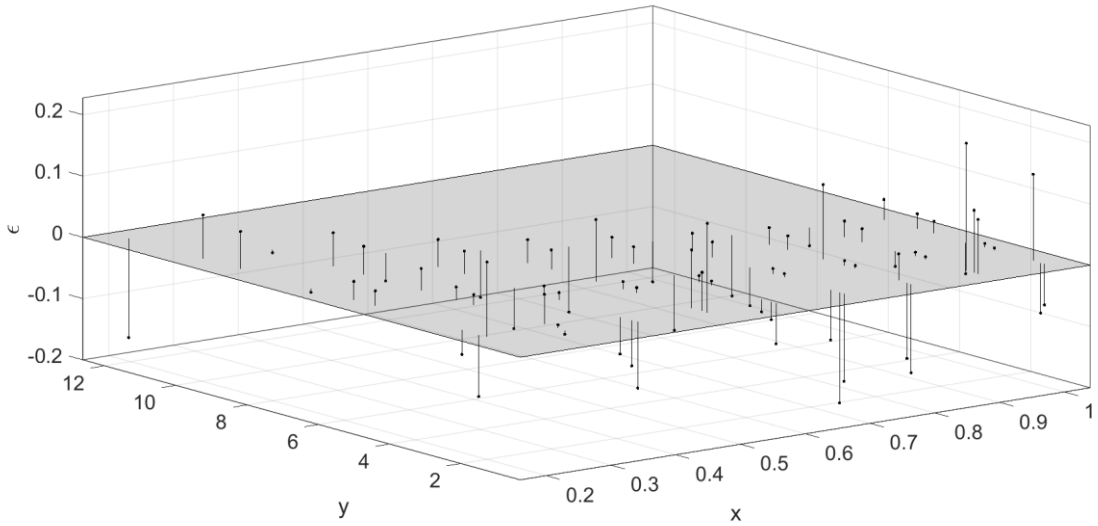

(b)

Figure 21. Fitting results: (a) surface, (b) residuals.

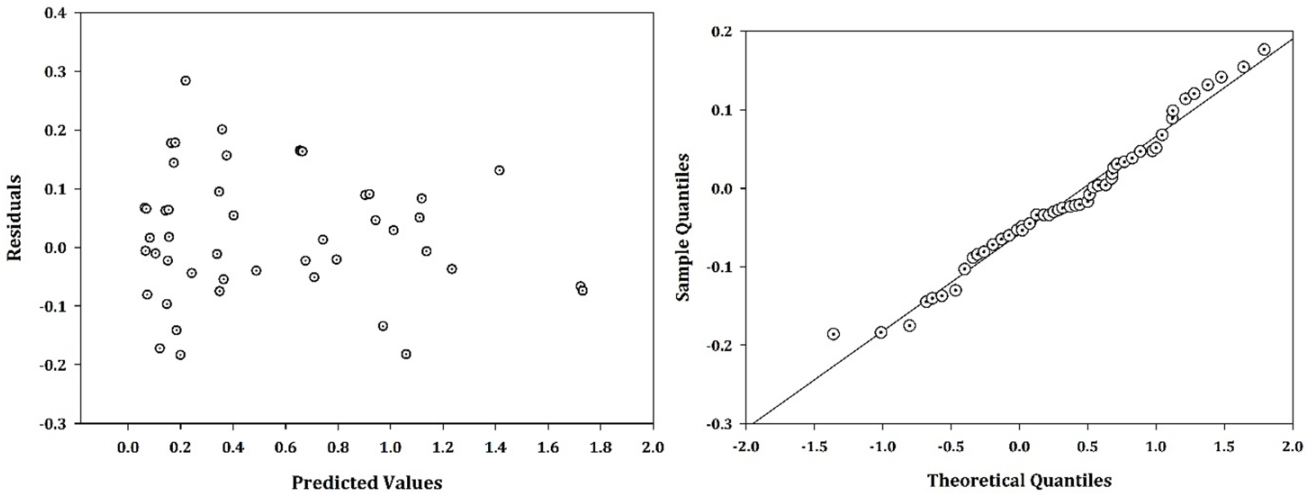

(a) (b)

Figure 22. Residual tests: (a) normality test, (b) homoscedasticity test.

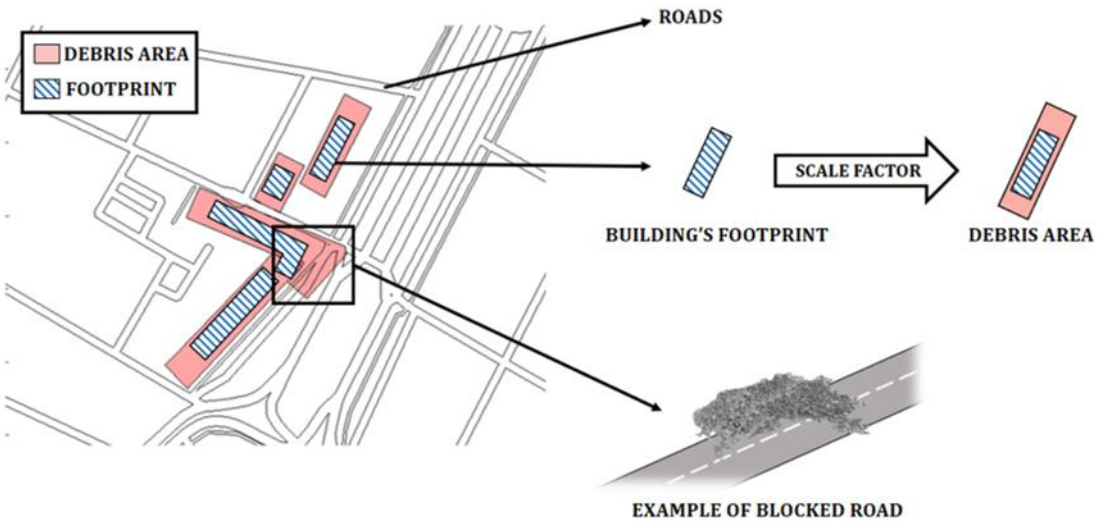

Figure 23. Building (debris) and transportation network (roads) interaction.